ADVANCED FUNCTIONAL MATERIALS

www.afm-journal.de

Liquid-Tin-Assisted Molten Salt Electrodeposition of Photoresponsive n-Type Silicon Films

*Junjun Peng, Huayi Yin, Ji Zhao, Xiao Yang, Allen J. Bard, and Donald R. Sadoway**

Production of silicon film directly by electrodeposition from molten salt would have utility in the manufacturing of photovoltaic and optoelectronic devices owing to the simplicity of the process and the attendant low capital and operating costs. Here, dense and uniform polycrystalline silicon films (thickness up to 60 µm) are electrodeposited on graphite sheet substrates at 650 °C from molten KCl–KF-1 mol% K_2SiF_6 salt containing 0.020–0.035 wt% tin. The growth of such high-quality tin-doped silicon films is attributable to the mediation effect of tin in the molten salt electrolyte. A four-step mechanism is proposed for the generation of the films: nucleation, island formation, island aggregation, and film formation. The electrodeposited tin-doped silicon film exhibits n-type semiconductor behavior. In liquid junction photoelectrochemical measurement, this material generates a photocurrent about 38–44% that of a commercial n-type Si wafer.

1. Introduction

Silicon is an attractive material for use in photovoltaic and optoelectronic devices.[1–8] While conventional manufacturing technology such as the Siemens process has seen great advances, there are still unmet needs in terms of high productivity and low cost for the aforementioned applications.[9] Direct fabrication of semiconductor thin films would possibly achieve new levels of efficiency and market penetration owing to process simplicity at lower capital and operating costs.[10] For example, hydrogenated amorphous silicon (a-Si:H) thin-film and polycrystalline Si thin-film solar cells are attractive for large-scale deployment of photovoltaics.[10–16] Currently, silicon thin films are mostly prepared by plasma-enhanced chemical vapor deposition,[10–12] in which a gaseous mixture of silane (SiH_4) and hydrogen deposit on glass, polymer, or metal a layer of amorphous or microcrystalline silicon measuring a few micrometers or less in thickness. Solid- or liquid-phase crystallization of amorphous silicon thin films by annealing or electron beam melting has been employed to obtain polycrystalline silicon thin films.[13–16] These techniques require elaborate equipment and high vacuum conditions resulting in low productivity and high cost.

Electrodeposition in molten salt has been considered as a candidate alternative method for preparation of polycrystalline silicon thin film due to the simplicity of the process offering the prospects of easy operation, low cost, and direct control of product quality and purity. By way of example, photoactive p-type silicon films, 3–10 µm thick, have been successfully electrodeposited on silver and graphite substrates in a melt of $CaCl_2$-nano-SiO_2.[17,18] However, due to the low solubility of SiO_2 in molten $CaCl_2$, it is difficult to form a film thicker than 10 µm which limits the improvement of the film quality. Electrodeposition of a thicker (>10 µm) silicon film on graphite or silver in a molten fluoride melted with K_2SiF_6 precursor had been realized in 1980s.[19–22] However, the electrodeposited silicon film was partially in the form of dendritic or spongy morphology. Moreover, owing to the low solubilities of LiF and NaF in water, it is difficult to remove the adhered salt from the electrodeposited silicon films.[23] Recently, a water soluble KCl–KF salt was employed to prepare a thick (more than 50 µm) silicon film or silicon coatings by electrodeposition,[24–27] yet no photoresponse has been demonstrated. Since the solubility of K_2SiF_6 in KCl–KF at 650 °C is much higher than that of SiO_2 in $CaCl_2$ at 850 °C, in the present study the feasibility of preparing a thick (>10 µm) and dense silicon film with photoactivity on a sheet substrate in KCl–KF–K_2SiF_6 bath was investigated and a successful formulation was discovered.

Herein, electrodeposition of dense and photoactive silicon films in molten KCl–KF-1 mol% K_2SiF_6 salt at 650 °C on graphite sheet substrates has been demonstrated. For the first time, it is disclosed that in contrast to previously generated silicon nanowires in this system, with tin as liquid metal immersed in the molten salt, a dense, thick, and uniform silicon film can be prepared. The effects of tin concentration, current density, and deposition time on the morphology of the

Dr. J. J. Peng, Dr. H. Y. Yin, Dr. J. Zhao, Prof. D. R. Sadoway
Department of Materials Science and Engineering
Massachusetts Institute of Technology
Cambridge, MA 02139-4307, USA
E-mail: dsadoway@mit.edu

Dr. J. J. Peng
College of Chemistry and Chemical Engineering
Key Laboratory of Biomass Fibers and Eco-dyeing & Finishing
Wuhan Textile University
Wuhan 430200, P. R. China

Dr. H. Y. Yin
School of Metallurgy
Northeastern University
Shenyang 110819, P. R. China

Dr. X. Yang, Prof. A. J. Bard
Department of Chemistry
University of Texas
Austin, TX 78712, USA

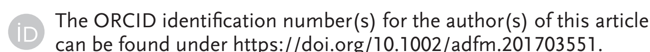
The ORCID identification number(s) for the author(s) of this article can be found under https://doi.org/10.1002/adfm.201703551.

DOI: 10.1002/adfm.201703551

© 2017 WILEY-VCH Verlag GmbH & Co. KGaA, Weinheim

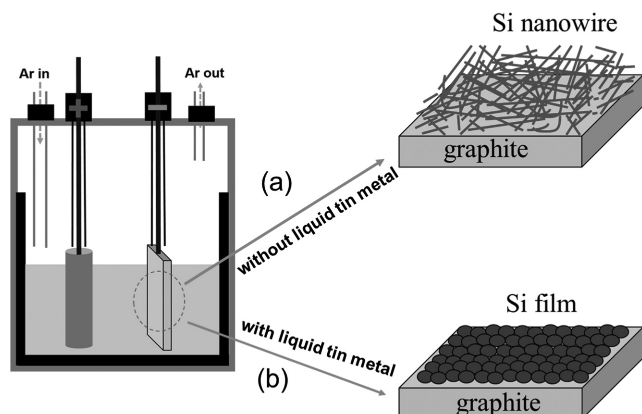

Figure 1. A schematic representation of silicon products with different morphologies on graphite sheet cathode electrodeposited in KCl–KF-1 mol% K_2SiF_6 molten salt: a) from tin-free molten salt and b) from molten salt containing tin.

electrodeposit have been investigated. The mechanism of tin-assisted electrodeposition of a dense silicon film in KCl–KF-1 mol% K_2SiF_6 was also proposed. Moreover, the photoresponse of the silicon films has been tested by a photoelectrochemical measurement.

2. Results and Discussion

A schematic representation of electrodeposition of silicon is illustrated in **Figure 1**. In a typical experiment, a two-electrode electrochemical cell (cathode: graphite sheet, rigid, or soft foil; anode: graphite rod) was operated galvanostatically at 650 °C. The electrolyte was a low eutectic mixture of KF and KCl, containing 1 mol% of K_2SiF_6. Addition of tin to the molten salt bath affected the morphologies of the silicon products deposited on the graphite substrate. When the molten salt was tin-free KCl–KF-1 mol% K_2SiF_6, the Si products on the graphite substrate were nanowires. However, if the bath contained 0.020–0.035 wt% tin, a dense silicon film could form.

Direct evidence was obtained by scanning electron microscopy (SEM), as shown in **Figure 2**. Samples were prepared under different deposition conditions in KCl–KF-1 mol% K_2SiF_6 salt at 650 °C, with and without tin. From the tin-free salt, yellow or brown powdery products were generated on the graphite substrate at cathodic current densities ranging from 5 to 50 mA cm^{-2}. The morphologies of two typical samples (Figure 2a,b) showed randomly oriented nanowires. These nanowire products were elemental silicon, verified by energy dispersive spectroscopy (EDS) and X-ray diffraction (XRD) (**Figure 3**). The mechanism of formation of silicon nanowires by electrodeposition in molten KF–KCl–K_2SiF_6 is not clear. In contrast, deposition from the same salt containing a tiny amount of tin (0.020–0.035 wt%) resulted in dense, blue-gray films on the surface of soft graphite foil or rigid graphite plate. The films consisted of crystal grains from several micrometers up to 50–70 µm (Figure 2c,e). A dense 10 µm thick film (Figure 2c,d) was produced by electrodeposition at 5 mA cm^{-2} for 4 h in a bath containing 0.02 wt% tin. A deposition time of more than 1.5 h is required to get a dense film fully covering the graphite substrate under these conditions. A series of dense films of different thickness obtained after electrolysis for 0.5–16 h is displayed in Figure S1 (Supporting Information), indicating a good linear correlation between thickness and deposition time. The current efficiencies of the electrodeposited silicon films from 2 to 16 h were in the range of 85–92%. Loss of current efficiency is attributed to the fact that the molten salt in contact with elemental metals will exhibit some degree of electronic conductivity. Moreover, parasitic reactions can reduce current efficiency. For example, since the distance between the anode and the cathode is small, recombination of the products of

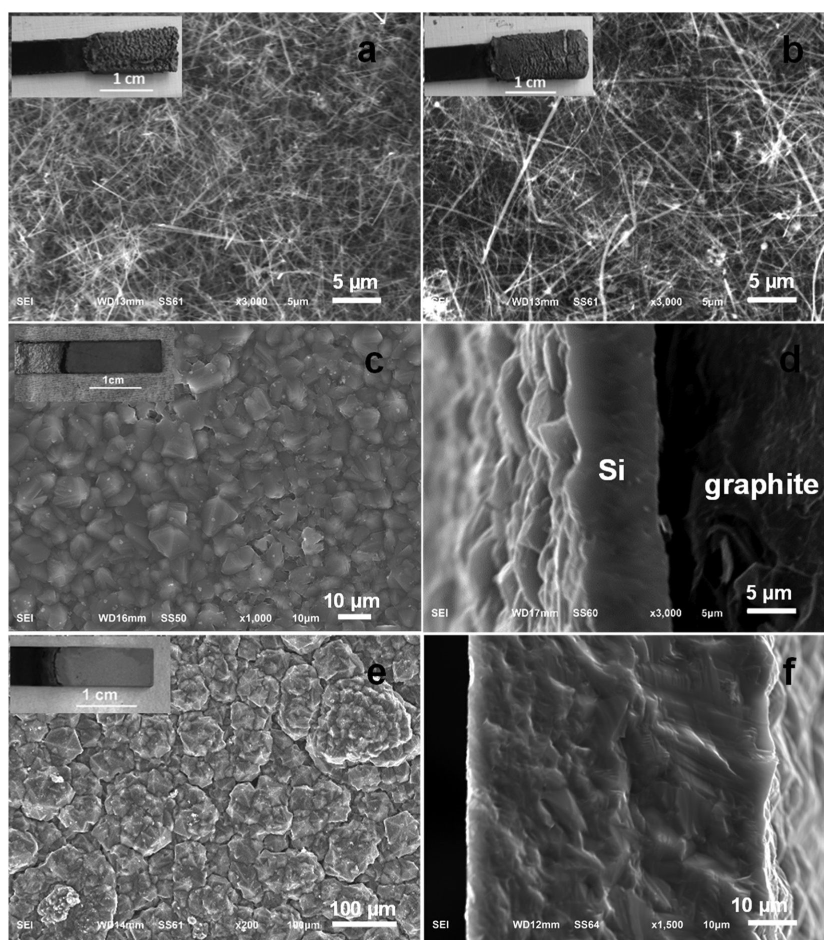

Figure 2. SEM images and corresponding photographs (the insets) of deposited products in KCl–KF-1 mol% K_2SiF_6 bath at 650 °C under different conditions as follows: graphite foil substrate, tin-free molten salt: a) 5 mA cm^{-2} for 4 h and b) 20 mA cm^{-2} for 4 h; c,d) graphite foil substrate, with 0.02 wt% tin in the molten salt, 5 mA cm^{-2} for 4 h; e,f) rigid graphite plate substrate, with 0.035 wt% tin in the molten salt, 20 mA cm^{-2} for 4 h.

© 2017 WILEY-VCH Verlag GmbH & Co. KGaA, Weinheim

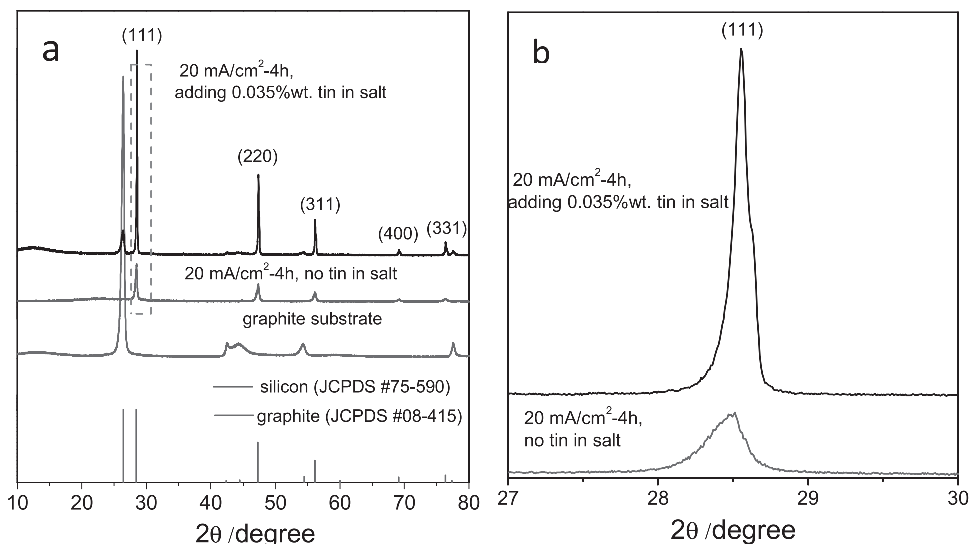

Figure 3. a) XRD patterns of electrodeposited products on rigid graphite substrate in KCl–KF-1 mol% K_2SiF_6 at 650 °C under different conditions as indicated. b) The magnified (111) peak in (a).

electrolysis is possible, i.e., the chlorine gas generated on the anode may find its way to the cathode where it can react.

EDS mapping (Figure S2, Supporting Information) of the cross-sectional profile of the film prepared at 5 mA cm^{-2} for 16 h revealed that the composition was dominantly silicon with a trace of tin, indicating that the film could be tin-doped silicon. The elemental carbon was detected as having been incorporated into the interface between the graphite substrate and silicon film, the thickness of this region ≈2–3 µm. The concentration of tin in the film was in the range from 0.4 to 2.2 wt% tuned by current density, time, and the concentration of tin in the melt (as shown in Table S1 in the Supporting Information). A thicker film (about 61 µm thickness) was produced on a rigid graphite plate substrate at 20 mA cm^{-2} for 4 h in a bath with 0.035 wt% Sn (Figure 2e,f). The tin-doped silicon film was strongly attached to the rigid substrate and could thus be polished to form a shiny mirror-like smooth surface without cracking or detaching (Figure S3, Supporting Information), which could be potentially useful for a device preparation.

Figure 3 shows the XRD results of typical samples deposited at 650 °C in KCl–KF-1 mol% K_2SiF_6 with and without tin. As seen in Figure 3a, the XRD patterns of the nanowires obtained at 20 mA cm^{-2}, 4 h, in tin-free bath match very well the standard diffraction peaks of silicon. Under the same deposition conditions but from a molten salt containing 0.035 wt% tin, the product (attached to the graphite substrate) was composed of silicon and graphite. The peak of film was more intense and sharper than that of nanowires, revealing good crystallinity for the tin-doped silicon film. The magnified peak (111) in Figure 3b clearly shows the difference between samples obtained with and without tin in the molten salt. Silicon nanowire has a broader peak with lower intensity, whereas tin-doped silicon film has a narrower peak with higher intensity, accompanied by a tiny rightward shift. The lattice parameter of the silicon film sample was calculated to be 5.411Å, which was slightly smaller than that of silicon nanowires sample, 5.430 Å. For the samples on graphite foil substrate, the XRD patterns of different films at 5 mA cm^{-2} from 1 to 16 h in Figure S4 (Supporting Information) reveal good crystallinity. The longer deposition time yielded better crystallinity (larger grains). This result agreed very well with SEM observations in Figure 1 and Figure S1 (Supporting Information).

Based on the above results, tin in KCl–KF-1 mol% K_2SiF_6 salt played a major role in the formation of dense film silicon. In order to investigate the effect of tin in the molten salt, cyclic voltammetry (CV) was performed on a graphite rod as working electrode in KCl–KF-1 mol% K_2SiF_6 bath with and without tin (**Figure 4**a). In both melts, a pair of reversible redox peaks was observed, ranging from –0.9 to –1.1 V versus graphite quasireference electrode. The reduction current starts increasing at –0.9 V and rises to a peak **c1** at –1.05 V, which we assigned to the electroreduction of SiF_6^{2-} to Si on graphite. Upon the reverse sweep, an oxidation peak **a1** can be observed at –0.73 V, which is due to anodic dissolution (oxidization) of deposited silicon. This behavior is similar to that observed by others on a silver electrode as substrate in LiF–KF–K_2SiF_6 or KCl–KF–K_2SiF_6.[23,24] However, in our molten salt containing 0.02 wt% tin, at more positive potentials, a new pair of redox waves was observed with a small cathodic peak **c2** at –0.4 V and a larger anodic peak **a2** at –0.25 V. These redox peaks should be related to the electrochemical reaction of tin. In order to confirm this, cyclic voltammetry was performed on a working electrode of liquid tin (tin contained in a boron nitride crucible, contacted by a Mo wire) (inset in Figure 4b) in KCl–KF-1 mol% K_2SiF_6. On the cathodic sweep, the redox couple, peaks **c3** and **a3**, was the same as those on the graphite electrode in Figure 4a, indicating that electrodeposition and stripping of silicon took place on a liquid tin metal substrate. More importantly, on the anodic sweep, a wave appeared at –0.3 V and the current gradually increased with positively shifting potential. This should be due to the electrooxidation of liquid tin to Sn^{2+} in molten salt, which matches the CV curves of a graphite rod in the salt with 0.02 wt% tin (black curve in Figure 4a). From the CVs, the Sn^{2+} in the molten salt electrolyte could come from the dissolution

© 2017 WILEY-VCH Verlag GmbH & Co. KGaA, Weinheim

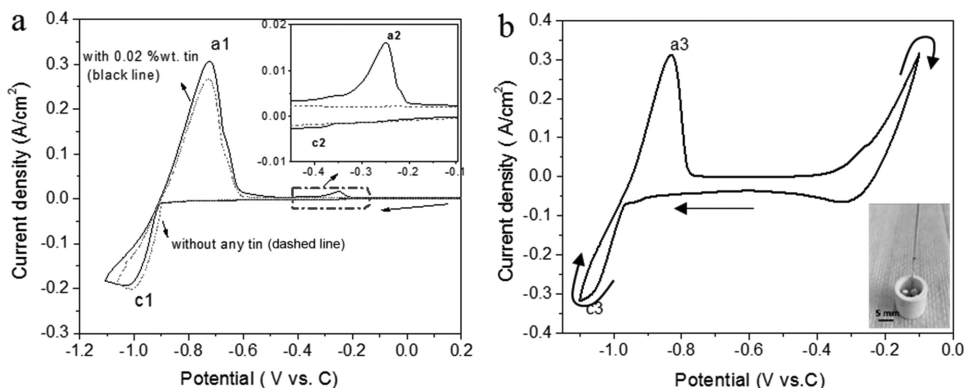

Figure 4. Cyclic voltammetry of different working electrodes: a) graphite rod working electrode at 650 °C in KCl–KF-1 mol% K_2SiF_6 salt with and without 0.02 wt% tin metals, and the inset is the magnification of the dashed box. Scan rate is 20 mV s^{-1}. b) Tin metal assembled in boron nitride crucible (shown in the inset) as working electrode in KCl–KF-1 mol% K_2SiF_6 salt. Scan rate is 20 mV s^{-1}.

of elemental Sn, its subsequent oxidation to Sn^{2+}, at a positively polarized electrode. Moreover, tin metal dissolved in the melt could also directly react with deposited silicon to form silicon-tin alloys. Ultimately, tin was codeposited with Si on the cathode, which could induce lateral growth of silicon film instead of undesirable nanowires.

In order to understand the growth process of tin-doped silicon film, the samples of different deposit time were collected and analyzed by SEM. Morphologies of samples corresponding to different growth stages are displayed in **Figure 5**, together with a schematic drawing of a four-step growth process. The first step, observed in the first 5 min at a cathodic current density of 5 mA cm^{-2}, results in a dispersion of discrete submicron particles rooted on the surface of the graphite substrate. This first step is nucleation (Figure 5a). For comparison, electrodeposition under the same conditions in KCl–KF-1 mol% K_2SiF_6 salt at 650 °C but without tin yielded very different results. The product was a yellow porous thin layer of silicon nanowires (Figure S5, Supporting Information). Returning to electrodeposition in the presence of dissolved tin, when the processing time extended up to 15 min, a large number of the previously nucleated particles had grown in size to the point of impingement to form islands measuring 5–10 µm in breadth. EDS mapping revealed that the islands consisted of silicon and tin (Figure S6, Supporting Information). This is the second step, named island formation and growth (Figure b). In this step, there are two contributors to island formation and growth: the attachment of new tin-doped silicon nucleus to the island and the surface diffusion of tin-doped silicon nuclei. With its dominantly metallic bonding tin is a better diffuser than covalently bonded silicon. Plus, on the basis of consideration of the processing temperature (650 °C) compared to the melting points of tin (232 °C) and silicon (1428 °C) one would expect tin to be far more mobile than silicon. Tin appears to act as a mediator for attaching silicon atoms and facilitating island lateral growth. Similar thin film growth behavior was verified

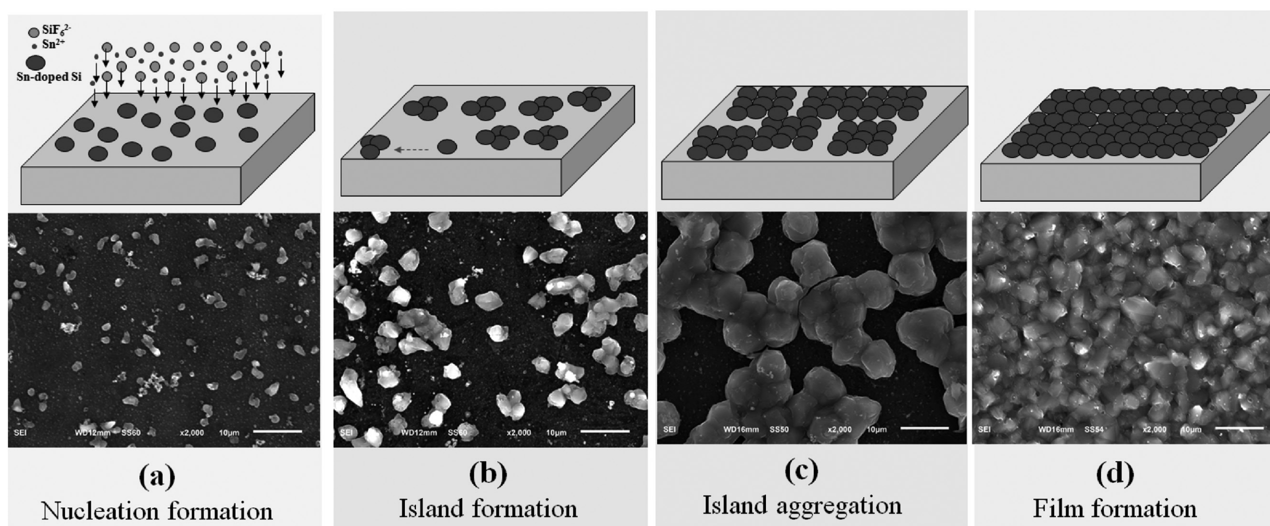

Figure 5. Schematic representation of growth process of tin-doped silicon film from electrodeposition on graphite foil substrate at 650 °C in KCl–KF-1 mol% K_2SiF_6 salt with 0.02 wt% tin metal and corresponding morphologies of samples with different time at 5 mA cm^{-2}: a) nucleation, in 5 min; b) island formation, in 15 min; c) island aggregation, in 30 min; and d) film formation, more than 90 min.

© 2017 WILEY-VCH Verlag GmbH & Co. KGaA, Weinheim

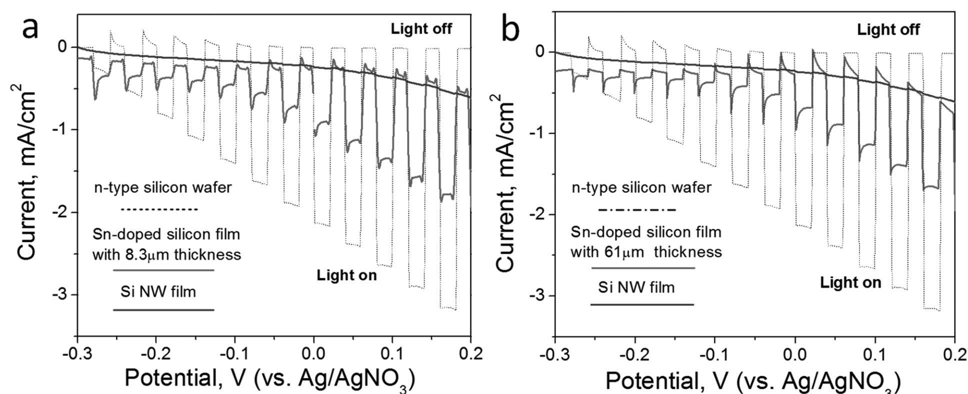

Figure 6. Photoresponse of Sn-doped silicon films with different thicknesses: a) 8.3 µm and b) 61 µm; silicon nanowire film and commercial n-type silicon wafer versus the applied potential with light on and off measured in a photoelectrochemical cell.

by electrochemical defect-mediated growth for silver/gold or copper films in aqueous solution.[28,29] When electrodeposition time increased to 30 min, tin-doped silicon islands were connected together and formed island aggregations (Figure 5c), named as the third step. Finally, as the time increased to 90 min, tin-doped silicon island aggregations continued to grow normal to the substrate and gradually formed a dense and coherent film. This step is denoted as film formation (Figure 5d).

The photoelectrochemical (PEC) measurement is a simple method to characterize the photoactivity of semiconductor materials without the need of forming solid/solid junctions.[17,18,30] The measurement was conducted in an acetonitrile solution containing 0.1 M tetrabutylammonium hexafluorophosphate ($TBAPF_6$) as the supporting electrolyte. 0.05 M ferrocene was added as a redox reagent. The silicon films were immersed in the electrolyte to form a semiconductor/liquid junction. Occurrence of redox reaction at the interface generated photocurrent when the films were irradiated with UV–vis light at 100 mW cm^{-2}. **Figure 6** shows a recording of photocurrent for the silicon films versus the applied potential. Measurements were made on the Sn-doped silicon film of 8.3 µm thickness obtained by electrodeposition at 10 mA cm^{-2} for 2 h, a silicon nanowire coating film on rigid graphite substrate, and a commercial n-type polycrystalline silicon wafer. An increased anodic photocurrent corresponding to the oxidation of ferrocene of the Sn-doped silicon film under illumination with a potential shift in the positive direction was observed, identical to that of a commercial n-type polycrystalline silicon wafer, showing that the electrodeposited silicon is n-type. According to glow discharge mass spectrometry (GDMS) analysis (shown in Table S2, Supporting Information), there is elemental phosphorus in the film, so we suspect that the n-type behavior of Si is due to the presence of the supervalent dopant. For comparison, silicon nanowire film on the graphite substrate was also tested and no photocurrent was observed, indicating that the silicon nanowire film was not photoactive. The net photocurrent of Sn-doped silicon film of thickness 8.3 µm (Figure 6a) at 0.13 V was 1.26 mA cm^{-2}, which was about 44.1% that of the commercial n-type silicon wafer. For a thicker film with 61 µm (Figure 6b), its net photocurrent at 0.13 V was about 1.1 mA cm^{-2}, which was about 38.5% that of n-type silicon wafer. The failure of the photoresponse current to increase with increasing thickness could be due to the higher recombination current in the thicker film. The values of 44.1% and 38.5% that of n-type silicon wafer seem to be good. But they are still lower than that of a commercial n-type wafer. Dark current is observed in Figure 6, indicating undesired pinholes or cracks in the film. Therefore, the film quality needs further improvement. Moreover, it is worth exploring how other liquid metals, such as Bi, In, Ga, and Sb, affect the formation of dense silicon film for photovoltaic applications by electrodeposition from molten salt.

3. Conclusion

Dense and uniform Sn-doped silicon films were prepared on graphite sheet substrates by electrodeposition at 650 °C from molten KCl–KF-1 mol% K_2SiF_6 containing 0.020–0.035 wt% tin. At cathodic current densities ranging from 5 to 20 mA cm^{-2}, the thickness of electrodeposited the Sn-doped silicon film varied from 5 to 60 µm. Tin in the molten salt seems to act as a mediator facilitating the growth of a dense Sn-doped silicon film for which a four-step growth mechanism comprising nucleation, island formation, island aggregation, and film formation is proposed. The Sn-doped silicon film was photoactive, the PEC photocurrent measured to be about 38–44% that of a commercial n-type polycrystalline silicon wafer.

4. Experimental Section

Cyclic Voltammetry and Constant Current Electrolysis: A graphite crucible was filled with low eutectic mixture of potassium fluoride (>99.5%, BioUltra, Sigma-Aldrich, 52.3 g) and potassium chloride (>99%, anhydrous, Sigma-Aldrich, 82 g) (the mole ratio of KF and KCl is 0.45/0.55), containing 1 mol% K_2SiF_6 (>99.5%, Sigma-Aldrich, 4.5 g) as the silicon precursor. The crucible with the salt was sealed in a stainless steel test vessel. First, the test vessel was dried at 200 °C for 24 h and 450 °C for 12 h under vacuum. Later Ar gas was flowed and temperature was ramped to 650 °C at 2 °C min^{-1} to melt the salt. A tiny amount of tin metal powder (100 mesh, 99.995% metals basis, Alfa Aesar) was added to the molten salt at concentrations in the range of 0–0.07 wt%. A three-electrode system was used to perform CV by using as the working electrode either a graphite rod or liquid tin metal assembled in a boron nitride crucible, a graphite rod counter electrode, and a graphite quasireference electrode. Constant current electrolysis was performed

 © 2017 WILEY-VCH Verlag GmbH & Co. KGaA, Weinheim

between a graphite sheet cathode (graphite foil, 1.8 cm^2 or Poco graphite plate, 2.6 cm^2) and a graphite rod anode at a cathodic current density ranging from 5 to 50 mA cm^{-2}. The melt was preelectrolyzed at 5 mA cm^{-2} for 8–14 h. When the electrolysis was terminated, the graphite cathode was taken out of the molten salt and cooled in the headspace of the vessel protected by Ar. Finally, the sample was removed from the test vessel and washed with water to remove the salt, and the obtained deposit was dried at 80 °C for 10 h prior to further characterization.

PEC Measurement: The PEC measurement was performed in an Ar-purged acetonitrile (CH_3CN, 99%, Extra-dry, Acros, Fair Lawn, NJ) solution containing 0.1 mol L^{-1} tetrabutylammonium hexafluorophosphate ($TBAPF_6$, >99.9%, Fluka, Allentown, PA) as supporting electrolyte and 0.05 mol L^{-1} ferrocene (Sigma-Aldrich, St. Louis, MO) as redox reagent. A three-electrode setup was used to measure the photocurrent of the as-prepared Si film, oxide layer removed by HF solution. The counter electrode is a platinum wire and the reference electrode is $Ag/AgNO_3$ (0.01 mol L^{-1} in CH_3CN). An Xe lamp of incident light intensity of 100 mW cm^{-2} acted as a UV–vis light to irradiate the obtained Si working electrode. A commercial n-type polycrystalline silicon wafer (University Wafer with resistivity of 5–10 Ω cm) was also measured for comparison.

Equipment and Characterization: The as-prepared tin-doped silicon films were characterized by scanning electron microscopy (SEM, JEOL,) equipped with an X-ray gun for EDS and X-ray diffraction spectroscopy (X'Pert Pro, X-ray diffractometer equipped with Cu Kα radiation), glow discharge mass spectrometry (EAG Inc.).

Supporting Information

Supporting Information is available from the Wiley Online Library or from the author.

Acknowledgements

J.P. and H.Y. contributed equally to this work. The authors acknowledge the funding financial support by the Global Climate and Energy Project (GCEP Stanford Subaward Agreement No. 60853646-118146) and the China Scholarship Council Funding (201508420034). Any opinions, findings, and conclusions or recommendations expressed in this publication are those of the authors and do not necessarily reflect the views of Stanford University, the Sponsors of the Global Climate and Energy Project, or others involved with the Global Climate and Energy Project.

Conflict of Interest

The authors declare no conflict of interest.

Keywords

electrodeposition, liquid metal tin, molten salts, photoelectrochemistry, silicon films

Received: June 28, 2017
Revised: September 11, 2017
Published online:

[1] H. Águas, T. Mateus, A. Vicente, D. Gaspar, M. J. Mendes, W. A. Schmidt, L. Pereira, E. Fortunato, R. Martins, *Adv. Funct. Mater.* **2015**, *25*, 3592.
[2] D. Stüwe, D. Mager, D. Biro, J. G. Korvink, *Adv. Mater.* **2015**, *27*, 599.
[3] F. Priolo, T. Gregorkiewicz, M. Galli, T. F. Krauss, *Nat. Nanotechnol.* **2014**, *9*, 19.
[4] S. E. Han, G. Chen, *Nano Lett.* **2010**, *10*, 1012.
[5] M. Govoni, I. Marri, S. Ossicini, *Nat. Photonics* **2012**, *6*, 672.
[6] W. D. A. M. De Boer, D. Timmerman, K. Dohnalova, I. N. Yassievich, H. Zhang, W. J. Buma, T. Gregorkiewicz, *Nat. Nanotechnol.* **2010**, *5*, 878.
[7] B. Tian, X. Zheng, T. J. Kempa, Y. Fang, N. Yu, G. Yu, J. Huang, C. M. Lieber, *Nature* **2007**, *449*, 885.
[8] E. Garnett, P. Yang, *Nano Lett.* **2010**, *10*, 1082.
[9] S. Pizzini, *Sol. Energy Mater. Sol. Cells* **2010**, *94*, 1528.
[10] L. L. Kazmerski (Ed), *Polycrystalline and Amorphous Thin Films and Devices*, Academic Press, New York, NY **1980**.
[11] M. Rohde, M. Zelt, O. Gabriel, S. Neubert, S. Kirner, D. Severin, T. Stolley, B. Rau, B. Stannowski, R. Schlatmann, *Thin Solid Films* **2014**, *558*, 337.
[12] H. Huang, L. Lu, J. Wang, J. Yang, S. F. Leung, Y. Wang, D. Chen, X. Chen, G. Shen, D. Li, Z. Fan, *Energy Environ. Sci.* **2013**, *6*, 2965.
[13] C. Becker, D. Amkreutz, T. Sontheimer, V. Preidel, D. Lockau, J. Haschke, L. Jogschies, C. Klimm, J. J. Merkel, P. Plocica, S. Steffens, *Sol. Energy Mater. Sol. Cells* **2013**, *119*, 112.
[14] D. Amkreutz, J. Haschke, T. Häring, F. Ruske, B. Rech, *Sol. Energy Mater. Sol. Cells* **2014**, *123*, 13.
[15] J. Haschke, D. Amkreutz, L. Korte, F. Ruske, B. Rech, *Sol. Energy Mater. Sol. Cells* **2014**, *128*, 190.
[16] T. Matsuyama, N. Terada, T. Baba, T. Sawada, S. Tsuge, K. Wakisaka, S. Tsuda, *J. Non-Cryst. Solids* **1996**, *198*, 940.
[17] J. Zhao, H. Yin, T. Lim, H. Xie, H. Y. Hsu, F. Forouzan, A. J. Bard, *J. Electrochem. Soc.* **2016**, *163*, D506.
[18] S. K. Cho, F. R. F. Fan, A. J. Bard, *Angew. Chem., Int. Ed.* **2012**, *124*, 12912.
[19] D. Elwell, G. M. Rao, *J. Appl. Electrochem.* **1988**, *18*, 15.
[20] G. M. Rao, D. Elwell, R. S. Feigelson, *J. Electrochem. Soc.* **1980**, *127*, 1940.
[21] G. M. Rao, D. Elwell, R. S. Feigelson, *J. Electrochem. Soc.* **1981**, *128*, 1708.
[22] D. Elwell, R. S. Feigelson, G. M. Rao, *J. Electrochem. Soc.* **1983**, *130*, 1021.
[23] G. M. Haarberg, L. Famiyeh, A. M. Martinez, K. S. Osen, *Electrochim. Acta* **2013**, *100*, 226.
[24] K. Yasuda, K. Maeda, T. Nohira, R. Hagiwara, T. Homma, *J. Electrochem. Soc.* **2016**, *163*, D95.
[25] K. Maeda, K. Yasuda, T. Nohira, R. Hagiwara, T. Homma, *J. Electrochem. Soc.* **2015**, *162*, D444.
[26] K. Yasuda, K. Maeda, R. Hagiwara, T. Homma, T. Nohira, *J. Electrochem. Soc.* **2017**, *164*, D67.
[27] S. I. Zhuk, A. V. Isakov, A. P. Apisarov, O. V. Grishenkova, V. A. Isaev, E. G. Vovkotrub, Y. P. Zaykov, *J. Electrochem. Soc.* **2017**, *164*, H5135.
[28] K. Sieradzki, N. Dimitrov, *Science* **1999**, *284*, 138.
[29] S. Hwang, I. Oh, J. Kwak, *J. Am. Chem. Soc.* **2001**, *123*, 7176.
[30] H. Ye, H. S. Park, V. A. Akhavan, B. W. Goodfellow, M. G. Panthani, B. A. Korgel, A. J. Bard, *J. Phys. Chem. C* **2010**, *115*, 234.

© 2017 WILEY-VCH Verlag GmbH & Co. KGaA, Weinheim